Progress in Organic Coatings 179 (2023) 107506

Contents lists available at ScienceDirect

Progress in Organic Coatings

journal homepage: www.elsevier.com/locate/porgcoat

Stretchable and wash durable reactive silver ink coatings for electromagnetic interference shielding, Joule heating, and strain sensing textiles

Mingxuan Li [a], Mehdi Zarei [b], Anthony J. Galante [c], Brady Pilsbury [a], S. Brett Walker [d], Melbs LeMieux [d], Paul W. Leu [a,b,c,*]

[a] Department of Chemical Engineering, University of Pittsburgh, Pittsburgh, PA 15261, United States
[b] Department of Mechanical Engineering, University of Pittsburgh, Pittsburgh, PA 15261, United States
[c] Department of Industrial Engineering, University of Pittsburgh, Pittsburgh, PA 15261, United States
[d] 7901 East Riverside Drive, Bldg 1, Unit 150, Austin, TX 78744, United States

ARTICLE INFO

Keywords:
Durable conductive coating
Reactive ink
EMI shielding
Joule heating
Strain sensing

ABSTRACT

In this paper, we demonstrate a highly conductive, stretchable, and wash-durable fabric for a variety of electronic textile applications such as electromagnetic interference (EMI) shielding, Joule heating, and strain sensing by utilizing a chemical etchant pretreatment that promotes covalent bonding, a reactive silver ink with conformal in situ silver reduction, and the use of a polymer coating for a protective barrier. Reactive ink coated on polyethylene terephthalate (PET) knitted textiles exhibit an average EMI shielding efficiency of 74.8 dB in the X band (frequency range of 8–12 GHz) and 76.6 dB in the Ku band (12–18 GHz). The conductive textiles show high Joule heating performance, where a temperature of 152 °C can be achieved at only 1.3 V DC applied voltage. This Joule heating performance is maintained after stretching and washing. Furthermore, the textile may be used for strain sensing and monitoring human movement. As prepared silver films do not degrade after 1000 stretching cycles at 50 % strain and maintain EMI SE higher than 70 dB after 300 min washing. The demonstrated textiles may be used for wearable electronics, personal medical devices, and next generation communications.

1. Introduction

There has been great interest in electronic textiles (e-textiles) that integrate sensing, communications, and computing components directly into fabrics for applications in health, sports, fashion, and entertainment [1,2]. Towards this goal, there has been much interest in the incorporation of conductive materials into polymers [3–8]. This has included research into MX-enes [9,10], reduced graphene oxide [11], silver nanowires [2], gallium-based liquid metal droplets [12], and carbon nanotubes [13,14]. However, these materials tend to have poor electrical conductivity due to limitations in forming conductive pathways between materials. These materials also tend to have poor durability due to weak adhesion forces with underlying microfibers, which lead to materials separating from the microfibers during stretching or washing. It has been challenging to demonstrate textiles with high performance electronic capabilities and the durability to maintain device functionality after wear, stretching, and/or washing.

Various metal deposition methods such as sputter coating [15], electroplating [16] and plasma induced reduction [17] have been demonstrated to accommodate complex surface geometry and flexible substrates. However, these methods require vacuum with expensive equipment, which increases the fabrication cost [18–20]. MXenes have been reported to be able to achieve very high electromagnetic interference shielding efficiency (EMI SE) on textiles. Wang et al. reported MXene-decorated polyester textiles could achieve 90 dB EMI SE [10]. But the adhesion of this 2D material is a concern and its durability is questionable [21].

It has been reported that a liquid metal based conductive textile achieves 72.6 dB EMI SE and maintains 91.7 % of this performance after 5000 cycles of stretch and release [12]. However, washing is a harsher treatment and usually results in more significant degradation in EMI shielding performance [22]. Silver nanowire (AgNW) networks with a polyurethane (PU) protective layer on textile have demonstrated 63.9 dB SE and retained 89 % of this performance after 20 min washing cycles

* Corresponding author at: Department of Chemical Engineering, University of Pittsburgh, Pittsburgh, PA 15261, United States.
E-mail address: pleu@pitt.edu (P.W. Leu).

https://doi.org/10.1016/j.porgcoat.2023.107506
Received 20 December 2022; Received in revised form 11 February 2023; Accepted 17 February 2023
Available online 25 February 2023

[2]. Stretch- and wash-durable textiles with higher than 70 dB EMI SE after stretching and washing has yet to be demonstrated.

In this paper, we demonstrate the ability to fabricate highly conductive, stretchable, and washable fabrics. This was achieved due to the ability to conformally coat large thickness metal films onto polyethylene terephthalate (PET) fabric microfibers by increasing interfacial adhesion. KOH and $KMnO_4$ were used to etch the textile to increase the interfacial area and promote covalent bonding between the microfiber and silver. A chemical pretreatment of the textile microfibers etches the surface to increase interfacial area and functionalizes the surface to enable covalent bonding with the silver. Reactive silver inks provide for high conductivity without the voids present in nanoparticle-based inks [23–25]. The ink reduces in situ onto the microfibers and provides for conformal coverage. A final polydimethylsiloxane (PDMS) coating further enhances adhesion and provides for an additional protective barrier during washing. The as prepared etched PET, then silver coated, and finally PDMS coated textile (EPET-Ag-PDMS) can be used for three e-textile applications: high performance EMI shielding, Joule heating, and strain sensing. EMI shielding may be important for protecting the human body from harmful electromagnetic waves [26,27] or protecting electronic devices from surrounding radiation that may prevent devices from working accurately or used to access sensitive information [28]. The Joule heating effect has been widely used to generate heat via electrical power. This may be useful for clothing worn in cold environments [10]. This may also be useful for thermotherapy [29] or used to enhance the transdermal delivery of medicine [30]. Finally, strain sensing is of interest for measuring human motion and structural health monitoring [1,31].

EPET-Ag-PDMS exhibits an average EMI SE of 74.8 dB at frequency range of 8–12 GHz and 76.6 dB at 12–18 GHz. For Joule heating, a temperature of 152 °C can be achieved with only 1.3 V DC applied voltage. EPET-Ag-PDMS has better stretch and wash-durability than PET-Ag or EPET-Ag. The EPET-Ag-PDMS maintains EMI SE higher than 75 dB after 1000 stretch cycles at 50 % strain and EMI SE higher than 70 dB after 300 min of ultrasonic washing. EPET-Ag-PDMS heats up to 102 °C in 5 s at 1.3 V applied voltage and stabilizes at 152 °C. After removing the applied voltage, the textile cools down to 35 °C in 120 s. The achievable stable temperature is 139 °C after 1000 stretching cycles and 130 °C after 300 min washing. EPET-Ag-PDMS may also be utilized for sensing strain on the finger, wrist, and elbow through changes in resistance. EPET-Ag-PDMS has great potential in wearable electronics, heat management devices, and next generation smart mobile devices.

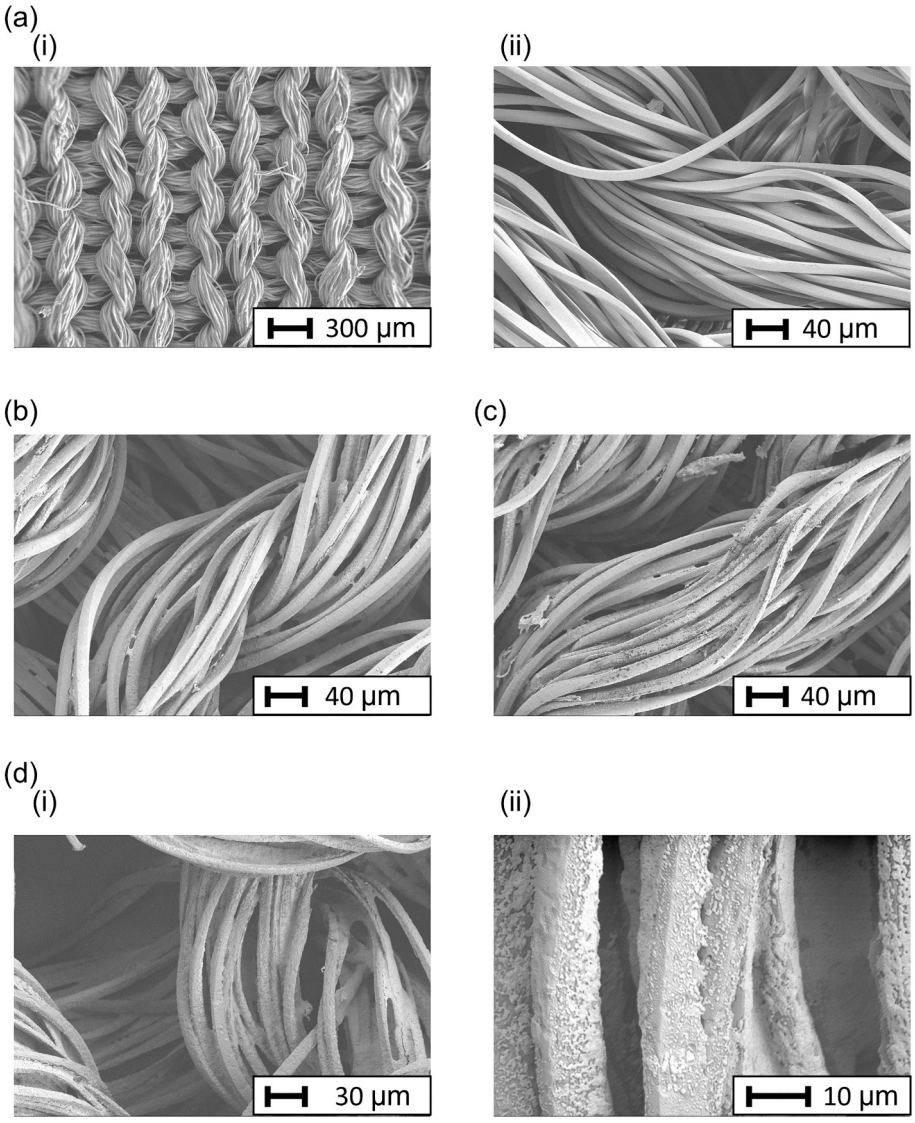

Fig. 1. SEM images of (a) knitted pattern for textile at (i) low and (ii) high resolution, (b) PET textile with two silver coats (PET-AG), (c) etched PET with two coats of Ag (EPET-Ag), and (d) etched PET textile with two coats of Ag followed by PDMS coating (EPET-Ag-PDMS) at (i) low and (ii) high resolution.

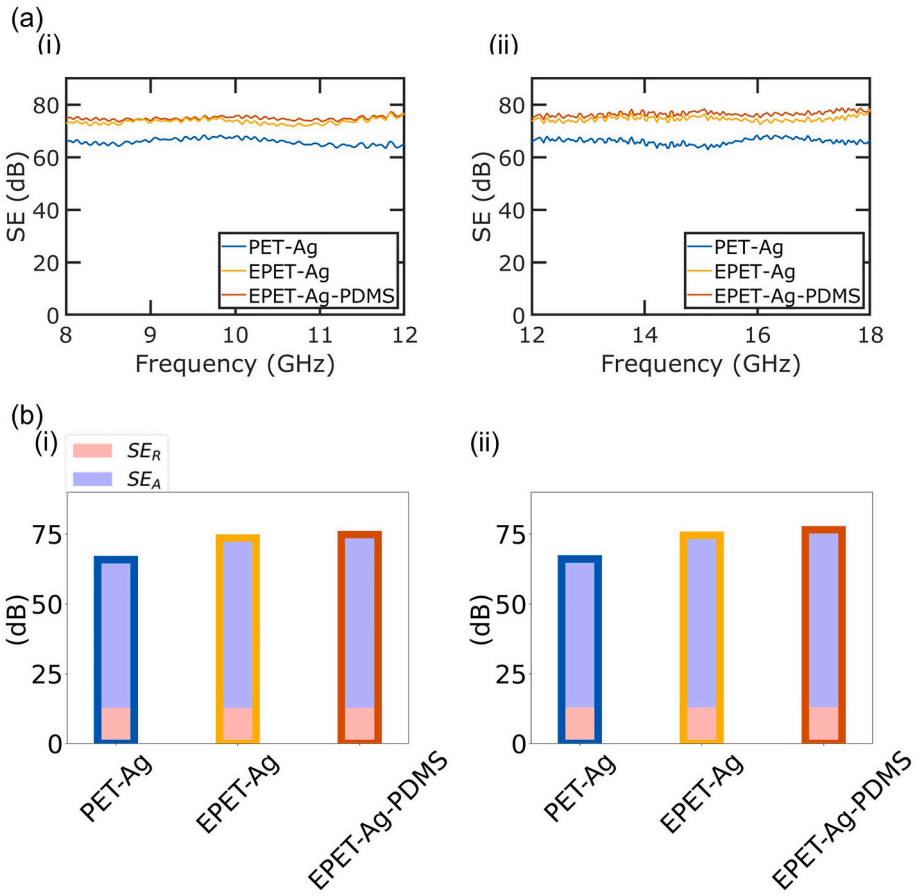

Fig. 2. (a) EMI SE for PET-Ag, EPET-Ag, and EPET-Ag-PDMS with two coating cycles. (b) Bar plot of averaged EMI SE_R, SE_A, SE for Two Ag coating cycles with different treatment at frequency range of (i) 8–12 GHz and (ii) 12–18 GHz.

2. Experimental section

2.1. Materials

Commercial flat stacked PET textile was bought from Anticon. Potassium hydroxide (KOH) water solution (45 %), potassium permanganate ($KMnO_4$, ACS reagent, ≥99.0 %), 2-Propanol (IPA, ACS reagent, ≥99.5 %), acetone (ACS reagent, ≥99.5 %), hexane (Laboratory Reagent, ≥95 %) and PDMS (Sylgard 184) were purchased from Sigma-Aldrich. The ink was prepared with silver acetate (CH_3COOAg, ReagentPlus, 99 %) and formic acid (HCOOH, ACS Reagent, ≥88 %) from Sigma-Aldrich by ElectronInks. Ammonium hydroxide (Certified A.C.S. Plus, 29.3 % assay) Extran MN 01 Powder was purchased from EMD Chemicals.

2.2. Sample preparation

2.2.1. Fabrication of EPET textile

PET fabric is cut into 2 cm × 2 cm pieces, rinsed by 50 ml isopropyl alcohol (IPA) and 50 ml acetone and then dried in oven at 40 °C overnight. Then, the as prepared PET fabric was chemically etched in 500 ml 45 % KOH water solution in a 1 l flask at 80 °C for 30 min. Then, a $KMnO_4$ solution was prepared with 500 mg $KMnO_4$ and 100 ml water. The PET fabric was then etched in 100 ml $KMnO_4$ water solution and heated at 80 °C for 30 min.

2.2.2. Fabrication of EPET-Ag textile

1 g of silver acetate was mixed with 2.5 ml of ammonium hydroxide in water for 15 s at room temperature. 0.2 mL of formic acid was titrated into the solution while constantly vortexing to mix the acid in. The color of the solution changed from light orange to gray and was allowed to settle overnight to precipitate large particles. The clarified supernatant was then decanted and filtered through a 200 nm syringe filter (Whatman Filters, Anotop 25) as reactive ink in the next step. 500 µl reactive silver ink was drop coated on the EPET textile, then it was cured in oven at 120 °C for 1 h.

2.2.3. Fabrication of EPET-Ag-PDMS textile

5 g PDMS (Sylgard 184) was mixed with 0.5 g curing agent into a 10 ml flask, and the mixture was stirred for 5 min until bubbles filled up the mixture. Then the mixture was degassed in a vacuum chamber for 30 min until there were no more bubbles. The mixture was diluted with 10 ml hexane to make a PDMS solution. EPET-Ag samples were dip coated with 500 µL of the as prepared PDMS solution and then cured in an oven at 150 °C for 1 h and then 40 °C overnight.

2.3. Characterization

The surface morphology was characterized by Zeiss SIGMA VP scanning electron microscope. Samples were coated with a Pd layer By Denton Sputter Coater at current = 30 mA for 40 s. EMI SE was measured by the coaxial transmitted line method. The HP 7822D vector network analyzer (VNA) was used to generate and detect signal. The sample was placed in between two waveguide flanges based on the desired frequency range. Screws and nuts were used to keep the two waveguide flanges stable. The X band and Ku band waveguide flange were bought from PASTERNACK. For Joule heating, DC power (NANKADF 30 V 10A Bench power supply) was used as power source, and alligator clips were used to connect with the textile. The temperature during joule heating was recorded by FLIR ONE PRO IR camera. Strain

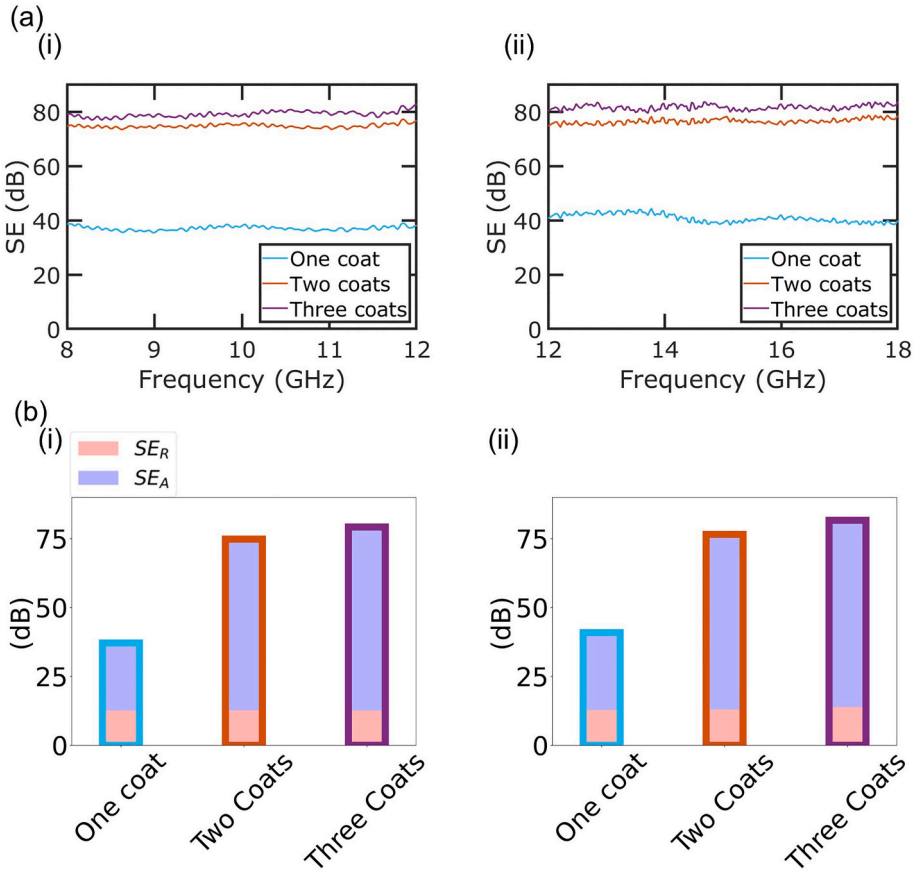

Fig. 3. (a) EMI *SE* for one, two, and three coats of Ag for EPET-Ag-PDMS textile. (b) Bar plot of averaged EMI SE_R, SE_A, SE for EPET-Ag-PDMS textile with different Ag coating cycles at frequency range of (i) 8–12 GHz (2) 12–18 GHZ.

sensing was performed by connecting the textile to the B1500A semiconductor Device Analyzer (Agilent Technologies) and recording the resistance when bending or moving.

2.4. Durability tests

2.4.1. Stretch test

Stretching was performed on PANAVISE 350 model stretch machine. For each stretching cycle, the textile was stretched to 50 % of its original length.

2.4.2. Wash test

Washing tests were performed by PowerSonic P230 Ultrasonic Cleaner under ASTM G13196 standards. 0.24 g Extran MN01 detergent powder was dissolved in 150 ml water and then transfered to centrifuge tubes where the sample were submerged by the detergent solution and then ultrasonicated at 44 °C. Then the sample was dried at oven at 120 °C until fully dry.

3. Result and discussion

3.1. Morphology of EPET-Ag-PDMS textile

Fig. 1 shows SEM images for different textile samples during processing. The knitted pattern of the PET textile is shown in Fig. 1(a) at (i) low and (ii) high resolution. Fig. 1(b) shows two Ag coatings on PET textiles directly (PET-Ag). It can be observed that Ag is uniformly coated on PET textile. Fig. 1(c) shows the etched PET textile with two coats of Ag (EPET-Ag). Fig. S1 shows SEM images at various resolutions comparing the PET with EPET. The increase in surface roughness due to etching can be seen in these SEM images. Compared to PET-Ag, the surface of EPET-Ag is not as smooth as PET-Ag as the chemical etching increases the surface roughness of the microfibers. Fig. 1(d) shows SEM images of PDMS coated on the EPET-Ag textile (EPET-Ag-PDMS) at (i) low and (ii) high resolution. The EPET-Ag is covered by a layer of PDMS to provide for a chemical protection layer.

3.2. EMI shielding effectiveness for different treatment

Fig. 2 shows the EMI SE for different treatment textiles at the frequency range of 8–12 GHz and 12–18 GHz. Fig. 2(a) compares the EMI SE of PET-Ag, EPET-Ag, EPETAg-PDMS using two Ag coating cycles. In Fig. 2(a), PET-Ag has an average EMI SE of 65.9 dB at 8–12 GHz and 66.1 dB at 12–18 GHz. EPET-Ag has an average EMI SE of 73.6 dB at 8–12 GHz and 74.6 dB at 12–18 GHz. EPET-Ag-PDMS has an average EMI SE of 74.8 dB at 8–12 GHz and 76.6 dB at 12–18 GHz.

The shielding efficiency SE is comprised of a reflection (SE_R) and an absorption component (SE_A) where SE = + SE_A. Fig. 2(b) plots the average SE_R and SE_A using bar plots which sum up to the average *SE* in the frequency range of (i) 8–12 GHz (ii) 12–18 GHz. SE_R as a function of frequency is plot in in Fig. S3. SE_R is approximately a constant in the two frequency ranges of 8–12 GHz and 12–18 GHz. Furthermore, SE_R does not vary between PET, EPET-Ag, and EPET-Ag-PDMS. In contrast, SE_A does change depending on processing. The average SE_A for PET-Ag, EPET-Ag, EPET-Ag-PDMS textiles with two Ag coats at a frequency range of 8–12 GHz are 53.2, 60.9, and 62.1 dB, respectively. In the 12–18 GHZ range, the SE is 53.2, 61.7, and 63.6 dB, respectively. The ratio of SE_A/SE in 8–12 GHz is 80.7 %, 82.7 %, and 83.0 % for PET-Ag, EPET-Ag, and EPET-Ag-PDMS, respectively. Etched PET increases Ag adhesion, so the thickness of the silver increases during the coating

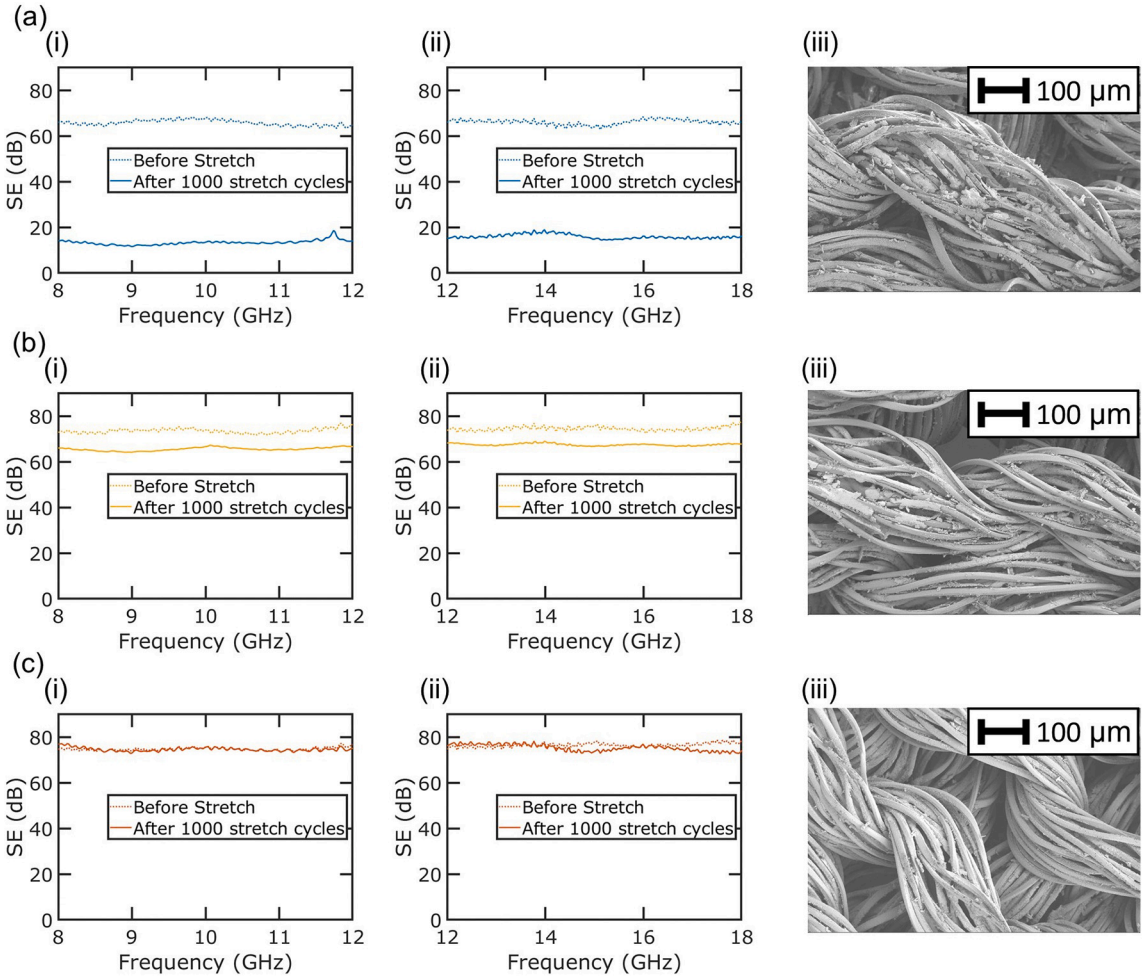

Fig. 4. Stretching tests for different treatment textile: (a) PET-Ag (b) EPET-Ag (c) EPET-Ag-PDMS. EMI SE at (i) 8–12 GHz (ii) 12–18 GHZ and (iii) SEM image after 1000 stretch cycles.

process. The Ag conductivity increases with increasing thickness since the coating is less influenced by surface scattering [6]. The Ag coating conductance increases and this increases the SE_A/SE ratio, and thus the overall *SE*. The change of SE is mainly due to the attenuation effect as noted by the increase in SE_A. However, an additional PDMS coating in EPET-Ag-PDMS does not increase the SE further as the PDMS coating does not affect the conductance of the underlying silver.

3.3. EMI shielding effectiveness for different Ag coating cycles

Fig. 3 shows the EMI SE as a function of number of coating cycles for EPET-Ag-PDMS. Fig. 3(a) shows the performance in the frequency range of (i) 8–12 GHz and (ii) 12–18 GHz. One coating of Ag has an average EMI SE of 37.1 dB from 8 to 12 GHz, and 40.9 dB from 12 to 18 GHz. Two coatings of Ag have an average EMI SE of 74.8 dB at 8–12 GHz and 76.6 dB at 12–18 GHz. Three coatings have an average SE of 79.2 dB at 8–12 GHz and 81.7 dB at 12–18 GHz. We decided to focus on two Ag coating cycles for electronic devices as the benefit in applying a third Ag coating is small in SE performance compared to that gained from adding a second coating. Fig. 3(b) plots the average SE_R and SE_A using bar plots which sum up to the average *SE* in the frequency range of (i) 8–12 GHz and (ii) 12–18 GHz. Fig. S1 plots SE_R as a function of frequency. SE_R does not vary with an increasing number of Ag coats. Neither the different types of treatment as discussed above nor the number of Ag coating cycles affects SE_R much. The average SE_A for one, two, and three coats of Ag for EPET-Ag-PDMS in the frequency range of 8–12 GHz are 24.5, 62.1, 66.6 dB, respectively. In the 12–18 GHZ range, SE_A is 28.1, 63.6, and 67.8 dB for one, two, and three coats of Ag, respectively.

The ratio of SE_A/SE for 8–12 GHz increases from 66.0 % to 83.0 % after the second coat, then to 84.1 % after the third coat. In the 12–18 GHz range, this ratio goes from 68.7 % to 83.0 % after the second coat, and then to 83.0 % after the third coat. When there is only one Ag coating, the ratio of SE_A/SE is lower since the conductivity is lower compared to more Ag coats. And when there are more coats, the conductivity increases and thus, the SE_A/SE ratio also increases.

3.4. Stretch durability

We performed stretch tests for different treatment samples and compared EMI SE before and after stretching. Stretching was performed on a PANAVISE 350 model stretch machine. For each stretching cycle, the textile was stretched to 50 % of its original length. SEM images were additionally used to evaluate the appearance of the coating after stretching. Fig. 4(a) shows the results of these stretch tests. The average EMI SE of PET-Ag changed from 65.9 to 13.3 dB in the 8–12 GHz and from 66.1 to 16.0 dB in the 12–18 GHz after 1000 stretch cycles. The SEM image in Fig. 4(a)(iii) shows the PET-Ag after 1000 stretch cycles. The Ag film is heavily peeled off from the microfibers due to poor adhesion. Fig. 4(b) shows the results for EPET-Ag. The average *SE* of EPET-Ag decreases from 73.6 to 65.6 dB in the 8–12 GHz range and from 74.6 to 67.6 dB in the 12–18 GHz range. The SEM image in Fig. 4(b)(iii) shows the EPET-Ag textile after 1000 stretch cycles. The Ag film is partially peeled off from the microfibers, but not as poorly as the PET-Ag. This is because the etch treatment increases adhesion by

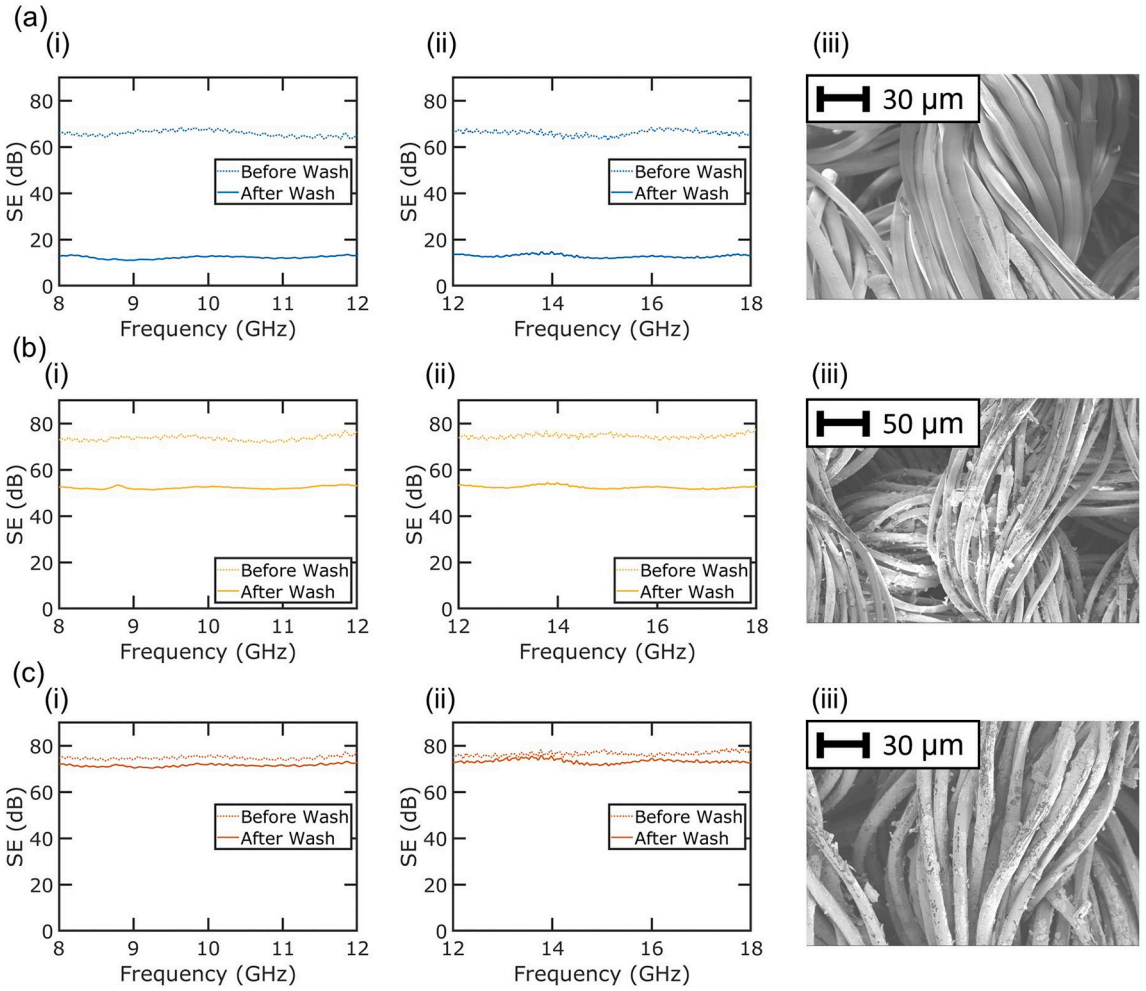

Fig. 5. Wash test for different treatment textile: (a) PET-Ag (b) EPET-Ag (c) EPETAg-PDMS. EMI SE at (i) 8–12 GHz (ii) 12–18 GHZ and (iii) SEM image after 300 min wash.

increasing the interfacial area between the silver and the microfiber as well as functionalizing the microfiber surface to strengthen the adhesion between the silver and the microfiber [32]. Fig. 4(c) shows results for the EPET-Ag-PDMS. The average SE changes from 74.8 to 74.7 dB in the 8–12 GHz range and from 76.6 to 75.4 dB in the 12–18 GHz range. The SEM image in (c)(iii) shows EPET-Ag-PDMS textile after 1000 stretch cycles. The Ag film appears pristine and just like it does prior to the stretch tests. Etching improves the adhesion of the Ag film to the microfiber, and the PDMS further improves this adhesion by additionally increasing the interfacial area of the silver and the microfiber and flexible PDMS. The PDMS fills in voids between the Ag and microfiber surface as well as providing an outer surface for silver adhesion.

3.5. Wash durability

Washing durability tests were performed on different treatment samples under ASTM G13196 standards for 300 min. After these washing tests, we measured the EMI SE and took SEM images on these samples. Fig. 5(a) shows PET-Ag results. The average *SE* decreases from 65.9 to 12.3 dB in 8–12 GHz and from 66.1 to 12.8 dB in 12–18 GHz. SEM image in (a)(iii) shows PET-Ag after 300 min washing. The Ag film is almost completely peeled off the microfibers. Fig. 5(b) shows results for EPET-Ag. The average EMI SE decreases from 73.6 to 52.3 dB in the 8–12 GHz range and from 74.6 to 52.5 dB in the 12–18 GHz range. The SEM image in 5(b)(iii) shows the EPET-Ag textile after 300 min washing, where the Ag film is partially peeled off from the microfibers. Fig. 5(c) shows results of EPET-Ag-PDMS. The SE decreases from 74.8 to 71.5 dB in 8–12 GHz and from 76.6 to 73.3 dB in 12–18 GHz. The SEM image in Fig. 5(c)(iii) shows the EPET-Ag-PDMS textile after 300 min washing. Although the Ag coating has some slight folds, it is still attached to the underlying microfiber due to protection of the PDMS layer. The PDMS effectively protects the Ag film even under harsh washing conditions by providing a chemical barrier that prevents the detergent solution from reacting with the Ag. Fig. S2 shows the EMI SE performance for PET coated with two coats of silver followed by PDMS coating (PET-Ag-PDMS). This sample is directly compared with the EPET-Ag-PDMS sample to demonstrate the impact of etching on performance and durability. EPET-Ag-PDMS has better performance than PET-Ag-PDMS as the etching increases the thickness of the silver coated on the PET textile. Furthermore, EPET-Ag-PDMS has better durability in EMI SE degradation compared to PET-Ag-PDMS under both stretching (Fig. 4c) and washing (Fig. 5c) as the etching provides for better Ag adhesion to the underlying PET.

3.6. Joule heating performance

Next we evaluated the Joule heating performance of the EPET-Ag-PDMS. According to Joule's Law, lower resistance enables high heating efficiency at lower applied voltages. This is not only better from an efficiency perspective, but also is safer due to the use of lower voltages. A 2 cm × 2 cm piece of EPET-Ag-PDMS textile was subject to different applied voltages U and the current I was recorded. The U–I curve

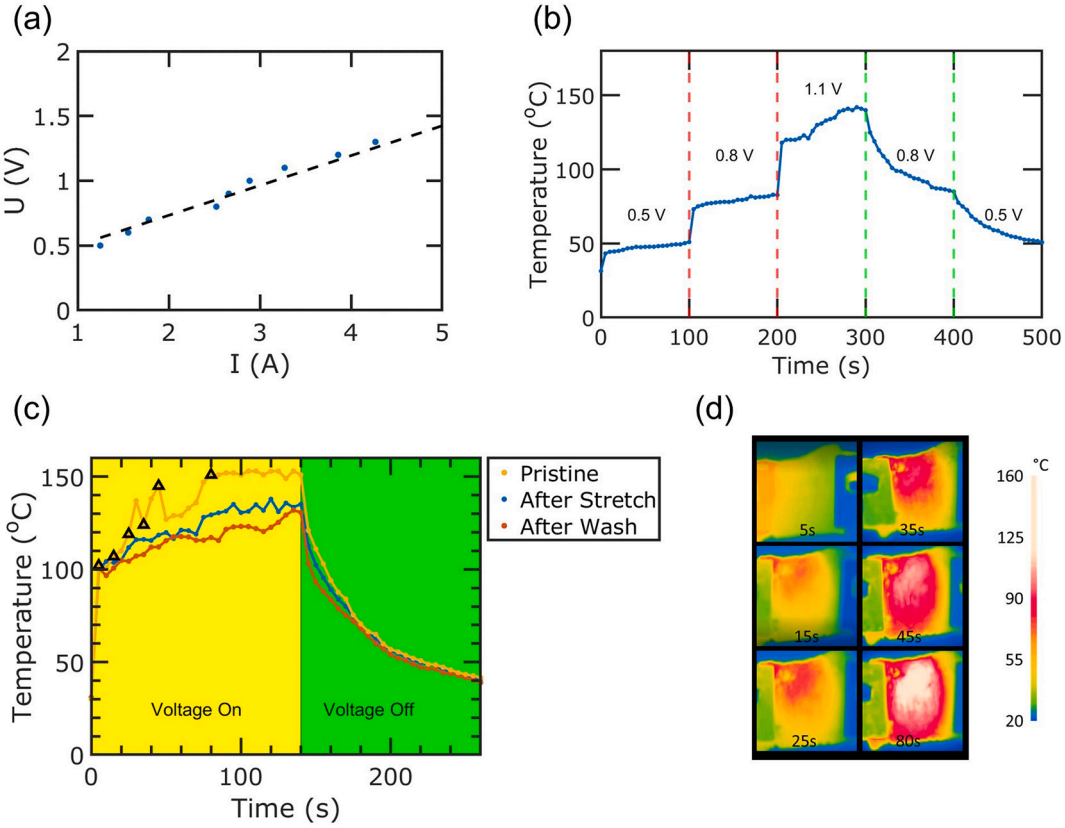

Fig. 6. Joule heating performance for EPET-Ag-PDMS textile: (a) U-I curve (b) Stepwise heating - cooling curve (c) Joule heating and cooling curve at 1.3 V for EPET-Ag-PDMS textile 1) Pristine 2) After Stretch 3) After Wash (d) Heat mapping of pristine EPET-AgPDMS textile at Voltage = 1.3 V at 5 s, 15 s, 25 s, 35 s, 45 s and 80s corresponding to black triangle in (c).

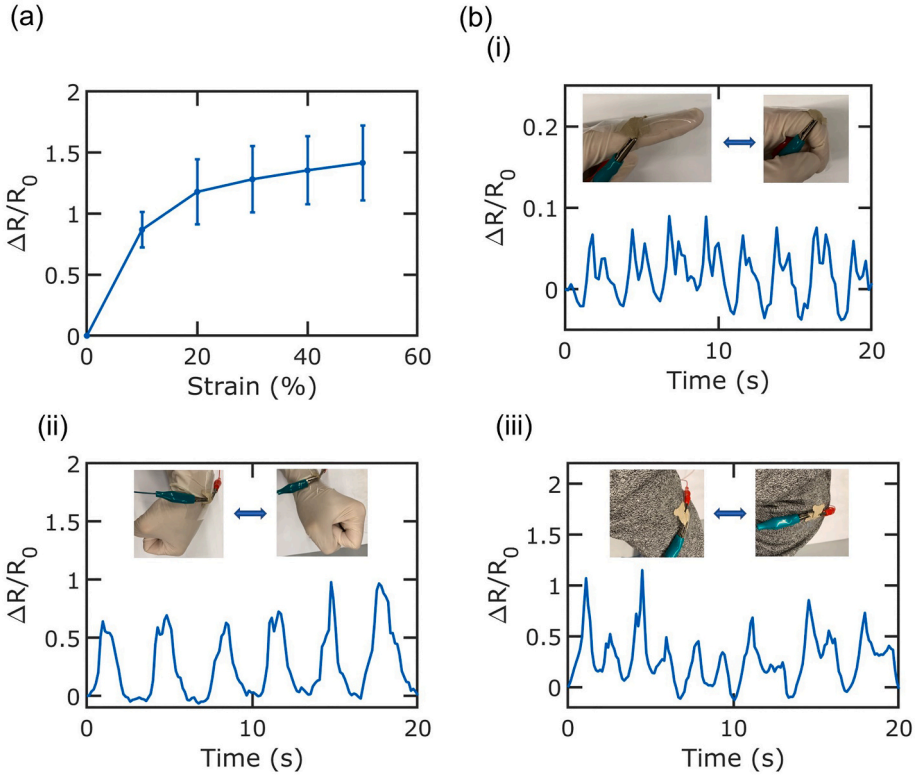

Fig. 7. (a) Strain- resistance change curve for EPET-Ag-PDMS textile (b) strain sensing signal for EPET-Ag-PDMS textile attached on (i) finger (ii) wrist (iii) elbow.

(Fig. 6a) indicates a very low resistance of as prepared sample. A prepared sample was heated and cooled stepwise to test the heating and cooling stability (Fig. 6b). For each heating/cooling step we waited 100 s to allow the temperature to stabilize. When the voltage applied was 0.5 V, the temperature stabilized at 50 °C. After increasing the voltage to 0.8 V, the temperature became 83 °C. When the voltage then increased to 1.1 V, the stable temperature was 142 °C. The voltage was then lowered to 0.8 V and the temperature gradually decreased to 85 °C after 100 s. After lowering the voltage to 0.5 V, the temperature cooled to 51 °C finally.

Fig. 6(c) shows the results of Joule heating performance tests of EPET-Ag-PDMS textile under pristine condition and then, after stretch and after wash tests. For each test, the voltage was applied for 140 s and then the voltage was removed for 120 s. Pristine samples heated up to 102 °C in 5 s and became stable at 152 °C. Then, they cooled down to 42 °C at the end. After stretching, samples heated up to 104 °C in 5 s and became stable at 139 °C. Then they cooled down to 39 °C at the end. After washing, samples heated up to 97 °C in 5 s and became stable at 130 °C. Then they cooled down to 37 °C at the end. Fig. 6(d) shows the temperature color map corresponding to the black triangle in (c), for 1.3 V voltage pristine EPET-Ag-PDMS textile after 5, 15, 25, 35, 45, and 80 s of heating. From the experiments above, the EPET-Ag-PDMS textile exhibits excellent Joule heating performance, where a stable temperature of 152 °C could be reached with only 1.3 V applied voltage. After 1000 stretch cycles, the stable heating temperature was maintained at 139 °C and after 300 min of ultrasonic washing the stable heating temperature was maintained at 130 °C, which indicates high wash durability for the joule heating application.

3.7. Strain sensing performance

We also demonstrate that the reactive silver ink treatment enables textile strain sensing. Strain sensing has been considered as an important application on wearable smart devices [31]. As strain is applied to the textile due to movement, the resistance of the textile changes accordingly, and can be used to monitor and capture movement. Because different bending patterns will cause the resistance signal to change differently, we can leverage this to distinguish which movements people are making by analyzing the resistance-time signal. In Fig. 7(a), we used the resistance change (ΔR) divided by the initial resistance (R_0) to characterize the strain. As the S\strain increased from 0 % to 60 %, the resistance change increased from 0 to 1.42, which confirmed the sensing capability of as prepared textile. Fig. 7(b)(i) shows the signal of 8 finger bending cycles. The finger movement is shown in the inset image. Fig. 7(b)(ii) shows the signal for wrist bending as the wrist goes from extension to flexion. The strain is larger than that of finger bending. Fig. 7(b)(iii) shows the signal when the elbow goes from extension to flexion. The strain here is the largest of the three types of movements studied. The noise measured can be mitigated by signal processing after analog to digital conversion. Noise can also be reduced by using a Wheatstone bridge, which improves the accuracy and stability of strain sensing compared to the simple two-terminal resistor demonstrated here.

4. Conclusion

In conclusion, we report a stretching and washing durable Ag coating method on textile with high EMI SE, good joule heating performance and strain sensing capability. A reactive ink was used with chemical etching pre-treatment and PDMS post-treatment to increase the adhesion of the Ag film to the fiber. The resulting EPET-Ag-PDMS textile exhibited a high average EMI SE of 74.8 dB at frequency range of 8–12 GHz and 76.6 dB at 12–18 GHz. The *SE* contribution was compared between reflection and absorption. It was observed that etch treatment on textile and increase the Ag coating cycles increases the shielding efficiency from absorption. Stretching tests were performed to compare different treatment. It was observed that etching and PDMS protection enable textile better durability over stretching. EPET-Ag-PDMS textile maintained EMI SE higher than 75 dB after 1000 stretch cycles of 50 % strain. With the protection of PDMS, EPET-Ag-PDMS textile also exhibited good washing durability. Samples maintained EMI SE higher than 70 dB after 300 min ASTM G131-96 standard washing. Excellent conductivity enabled high joule heating performance. EPET-Ag-PDMS textiles became stable at 152 °C at 1.3 V voltage input and cooled down to 35 °C in 120 s. This performance was demonstrated to be stretching and washing durable. In addition, strain sensing capability was demonstrated by attaching the EPET-Ag-PDMS textile on the finger, wrist, and elbow and then monitoring resistance. Our coating method demonstrates a simple, scaleable coating method for durable high EMI SE textile, which has great potential in wearable electronic, heat management devices and next generation smart mobile device.

CRediT authorship contribution statement

Mingxuan Li: Conceptualization, Methodology, Visualization, Investigation, Writing- Original draft preparation.
Mehdi Zarei: Data curation, Validation.
Anthony J Galante: Investigation, Validation.
Brady Pilsbury: Investigation.
S. Brett Walker: Methodology.
Melbs LeMieux: Supervision, Funding acquisition.
Paul W Leu: Supervision, Writing- Reviewing and Editing.

Declaration of competing interest

The authors declare the following financial interests/personal relationships which may be considered as potential competing interests: Paul W Leu reports financial support was provided by National Science Foundation.

Data availability

Data will be made available on request.

Acknowledgement

The authors thank Dr. Sneh Sinh for helpful discussions. The authors acknowledge support from the MDS-Rely Center to conduct this research. The MDS-Rely Center is supported by the National Science Foundation's Industry–University Co- operative Research Center (IUCRC) Program under award EEC-2052662 and EEC-2052776.

Appendix A. Supplementary data

SEM of PET and EPET textile, durability of PET-Ag-PDMS, Figures and discussion of SE_R. Supplementary data to this article can be found online at https://doi.org/10.1016/j.porgcoat.2023.107506.

References

[1] J. Wang, C. Lu, K. Zhang, Textile-based strain sensor for human motion detection, Energy Environ. Mater. 3 (2020) 80–100.
[2] L.-C. Jia, K.-Q. Ding, R.-J. Ma, H.-L. Wang, W.-J. Sun, D.-X. Yan, B. Li, Z.M. Li, Highly conductive and machine-washable textiles for efficient electromagnetic interference shielding, Adv. Mater. Technol. 4 (2019), 1800503.
[3] W. Zhang, A.A. Dehghani-Sanij, R.S. Blackburn, Carbon based conductive polymer composites, J. Mater. Sci. 42 (2007) 3408–3418.
[4] J. Chen, Y. Zhu, J. Huang, J. Zhang, D. Pan, J. Zhou, J.E. Ryu, A. Umar, Z. Guo, Advances in responsively conductive polymer composites and sensing applications, Polym. Rev. 61 (2021) 157–193.
[5] H. Liu, Q. Li, S. Zhang, R. Yin, X. Liu, Y. He, K. Dai, C. Shan, J. Guo, C. Liu, et al., Electrically conductive polymer composites for smart flexible strain sensors: a critical review, J. Mater. Chem. C 6 (2018) 12121–12141.
[6] M. Li, S. Sinha, S. Hannani, S.B. Walker, M. LeMieux, P.W. Leu, Ink-coated silver films on PET for flexible, high performance electromagnetic interference shielding and joule heating, ACS Appl. Electron. Mater. (2022) 173–180.

[7] Y. Wang, H.-K. Peng, T.-T. Li, B.-C. Shiu, X. Zhang, C.-W. Lou, J.-H. Lin, Layerby-layer assembly of low-temperature in-situ polymerized pyrrole coated nanofiber membrane for high-efficiency electromagnetic interference shielding, Prog. Org. Coat. 147 (2020), 105861.
[8] M.K. Yazdi, B. Noorbakhsh, B. Nazari, Z. Ranjbar, Preparation and EMI shielding performance of epoxy/non-metallic conductive fillers nano-composites, Prog. Org. Coat. 145 (2020), 105674.
[9] P. Wang, L. Yang, J. Ling, J. Song, T. Song, X. Chen, S. Gao, S. Feng, Y. Ding, V. Murugadoss, et al., Frontal ring-opening metathesis polymerized polydicyclopentadiene carbon nanotube/graphene aerogel composites with enhanced electromagnetic interference shielding, Adv. Compos. Hybrid Mater. 5 (2022) 2066–2077.
[10] Q.-W. Wang, H.-B. Zhang, J. Liu, S. Zhao, X. Xie, L. Liu, R. Yang, N. Koratkar, Z.-Z. Yu, Multifunctional and water-resistant MXene-decorated polyester textiles with outstanding electromagnetic interference shielding and joule heating performances, Adv. Funct. Mater. 29 (2019), 1806819.
[11] A.P. Godoy, L.G. Amurim, A. Mendes, E.S. Goncalves, A. Ferreira, C.S. de Andrade, R. Kotsilkova, E. Ivanov, M. Lavorgna, L.A. Saito, et al., Enhancing the electromagnetic interference shielding of flexible films with reduced graphene oxidebased coatings, Prog. Org. Coat. 158 (2021), 106341.
[12] L.-C. Jia, X.-X. Jia, W.-J. Sun, Y.-P. Zhang, L. Xu, D.-X. Yan, H.-J. Su, Z.M. Li, Stretchable liquid metal-based conductive textile for electromagnetic interference shielding, ACS Appl. Mater. Interfaces 12 (2020) 53230–53238. PMID: 33179903.
[13] H. Cheng, Y. Pan, X. Wang, C. Liu, C. Shen, D.W. Schubert, Z. Guo, X. Liu, Correction to: ni Flower/MXene-melamine foam derived 3D magnetic/conductive networks for ultra-efficient microwave absorption and infrared stealth, Nano-Micro Lett. 14 (2022), 116-116.
[14] G. Karalis, L. Tzounis, E. Dimos, C.K. Mytafides, M. Liebscher, A. KarydisMessinis, N.E. Zafeiropoulos, A.S. Paipetis, Printed Single-Wall carbon nanotube-based joule heating devices integrated as functional laminae in advanced composites, ACS Appl. Mater. Interfaces 13 (2021) 39880–39893. PMID: 34378907.
[15] H. Wang, C. Ji, C. Zhang, Y. Zhang, Z. Zhang, Z. Lu, J. Tan, L.J. Guo, Highly transparent and broadband electromagnetic interference shielding based on ultrathin doped ag and conducting oxides hybrid film structures, ACS Appl. Mater. Interfaces 11 (2019) 11782–11791.
[16] K.A. Ohiri, N.M. Nowicki, T.J. Montalbano, M. Presley, N.S. Lazarus, Electroplating of aerosol jet-printed silver inks, Adv. Eng. Mater. 23 (2021), 2100362.
[17] H.-J. Oh, V.-D. Dao, H.-S. Choi, Electromagnetic shielding effectiveness of a thin silver layer deposited onto PET film via atmospheric pressure plasma reduction, Appl. Surf. Sci. 435 (2018) 7–15.
[18] J. Li, Y. Wang, G. Xiang, H. Liu, J. He, Hybrid additive manufacturing method for selective plating of freeform circuitry on 3D printed plastic structure, Adv. Mater. Technol. 4 (2019), 1800529.
[19] B. Blakey-Milner, P. Gradl, G. Snedden, M. Brooks, J. Pitot, E. Lopez, M. Leary, F. Berto, A. du Plessis, Metal additive manufacturing in aerospace: a review, Mater. Des. 209 (2021), 110008.
[20] O. Abdulhameed, A. Al-Ahmari, W. Ameen, S.H. Mian, Additive manufacturing: challenges, trends, and applications, Adv. Mech. Eng. 11 (2019), 1687814018822880.
[21] S. Zhu, M. Wang, Z. Qiang, J. Song, Y. Wang, Y. Fan, Z. You, Y. Liao, M. Zhu, C. Ye, Multi-functional and highly conductive textiles with ultra-high durability through 'green' fabrication process, Chem. Eng. J. 406 (2021), 127140.
[22] J. Wang, Q. Hu, J. Huang, J. Li, Y. Lu, T. Liang, B. Shen, W. Zheng, W. Song, Multifunctional textiles enabled by simultaneous interaction with infrared and microwave electromagnetic waves, Adv. Mater. Interfaces 9 (2022), 2102322.
[23] S.B. Walker, J.A. Lewis, Reactive silver inks for patterning high-conductivity features at mild temperatures, J. Am. Chem. Soc. 134 (2012) 1419–1421.
[24] E.S. Rosker, M.T. Barako, E. Nguyen, D. DiMarzio, K. Kisslinger, D.-W. Duan, R. Sandhu, M.S. Goorsky, J. Tice, Approaching the practical conductivity limits of aerosol jet printed silver, ACS Appl. Mater. Interfaces (2020) 29684–29691.
[25] Z. Zhou, S.B. Walker, M. LeMieux, P.W. Leu, Polymer-embedded silver microgrids by particle-free reactive inks for flexible high-performance transparent conducting electrodes, ACS Appl. Electron. Mater. 3 (2021) 2079–2086. Publisher: American Chemical Society.
[26] J.-H. Moon, Health effects of electromagnetic fields on children, Clin. Exp. Pediatr. 63 (2020) 422–428.
[27] J.C. Lin, Electromagnetic Fields in Biological Systems, Taylor & Francis, 2012.
[28] S. Geetha, K.K.S. Kumar, C.R.K. Rao, M. Vijayan, D.C. Trivedi, EMI shielding: methods and materials—a review, _eprint: J. Appl. Polym. Sci. 112 (2009) 2073–2086 https://onlinelibrary.wiley.com/doi/pdf/10.1002/app.29812.
[29] S. Wu, Z. Cui, G.L. Baker, S. Mahendran, Z. Xie, Y. Zhu, A biaxially stretchable and self-sensing textile heater using silver nanowire composite, ACS Appl. Mater. Interfaces 13 (2021) 59085–59091.
[30] S. Chatterjee, P.C.-L. Hui, C.-W. Kan, W. Wang, Dual-responsive (pH/temperature) pluronic F-127 hydrogel drug delivery system for textile-based transdermal therapy, Sci. Rep. 9 (2019) 1–13.
[31] S. Seyedin, P. Zhang, M. Naebe, S. Qin, J. Chen, X. Wang, J.M. Razal, Textile strain sensors: a review of the fabrication technologies, performance evaluation and applications, Mater. Horiz. 6 (2019) 219–249.
[32] A.J. Galante, M. Li, B. Pilsbury, M. LeMieux, Q. Liu, P.W. Leu, Achieving highly conductive, stretchable, and washable fabric from reactive silver ink and increased interfacial adhesion, ACS Appl. Polym. Mater. (2022) 5253–5260.